

Photoisomerization of Saccharin

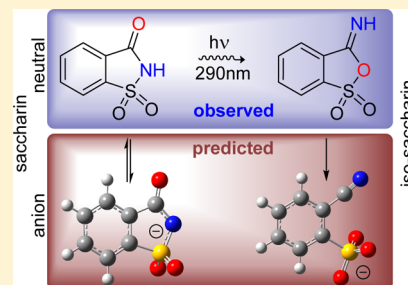
L. Duarte,[†] I. Reva,^{*,†} M. L. S. Cristiano,[‡] and R. Fausto[†]

[†]Department of Chemistry, University of Coimbra, P-3004-535 Coimbra, Portugal

[‡]CCMAR and Department of Chemistry and Pharmacy, University of Algarve, P-8005-139 Faro, Portugal

S Supporting Information

ABSTRACT: Most known applications of saccharin and saccharyl derivatives and their potential for new uses rely on the thermal and photochemical stability of the saccharyl system. Here, we show that saccharin undergoes structural rearrangement when subjected to a narrow-band ultraviolet irradiation. Monomeric saccharin was isolated in low-temperature argon matrices and its photochemistry was characterized by means of infrared spectroscopy and DFT calculations. Among several DFT methods used, the O3LYP/6-311++G(3df,3pd) level gave the best match with the experimental spectra. Irradiation of matrix-isolated saccharin, with a narrow-band source (290 nm), generates a so far unknown isomer that we call iso-saccharin. The structures of the conjugate bases of saccharin and iso-saccharin were also computed theoretically. Their free energies and dipole moments suggest that both anions may be relevant in systems where saccharin participates, as is the case of the recently proposed saccharin-based ionic liquids.

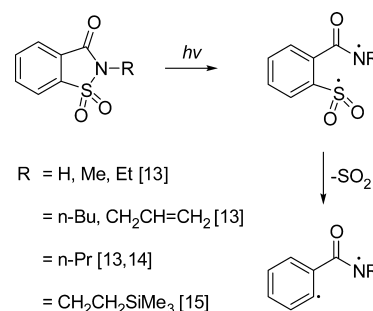


INTRODUCTION

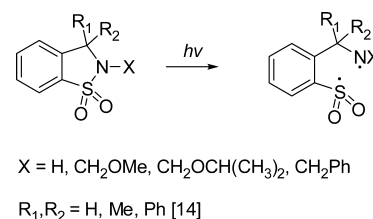
1,2-Benzisothiazol-3(2*H*)-one-1,1-dioxide (saccharin) and its derivatives have been extensively studied over the years, and in addition to their importance in the food industry,¹ they also find applications in the agricultural,² medical,³ and pharmaceutical areas.⁴ In organic and bioorganic synthesis, saccharin and saccharyl derivatives are known as cheap and versatile starting materials for the preparation of related heterocycles and as useful synthetic intermediates.⁵ Moreover, both saccharin and saccharinate act as ligands in coordination chemistry^{6,7} and have recently been considered for the formulation of amide-based ionic liquids.^{8–11} Most known applications of saccharin and saccharyl derivatives and their potential for new uses rely on the thermal and photochemical stability of the saccharyl system.

Regarding the photochemistry of benzisothiazoles, a literature search reveals that the information available is restricted to photolysis in solution. Early works on the photochemistry of *N*-propylsaccharin^{12,13} indicated that photolysis leads to cleavage of the S–N bond, ultimately resulting in formation of benzamide through extrusion of SO₂ (Scheme 1). Later, Döpp reported the photochemistry of 3,3-disubstituted 2,3-dihydro-1,2-benzisothiazole 1,1-dioxides in methanol and acetonitrile. Three reaction pathways were observed: in two cases, an initial S–N homolysis was suggested (Scheme 2) to be vital for these processes, and in the third, a formal oxygen shift from S to N, generating cyclic *N*-hydroxysulfonamides (sulfine hydroxamic acids), was proposed.¹⁴ Recently, Yoon, Mariano, and co-workers studied the photochemistry of *N*-[(trimethylsilyl)alkyl]saccharins in solution, reporting that, upon excitation, these compounds are involved in competitive silyl group transfer, homolysis of the S–N bond (Scheme 1), and H-abstraction processes, the relative contribution of each pathway depending on the

Scheme 1



Scheme 2



reaction conditions.¹⁵ Thus, the photochemistry of saccharyl derivatives in solution appears to be determined by the structure of the saccharyl ring, the nature of the substituents, and the reaction media. However, to the best of our knowledge, no information regarding the photochemistry of monomeric saccharin or its anion (conjugate base) is available.

In the present work, we report the photoisomerization of saccharin isolated in solid argon and discuss possible

Received: January 28, 2013

Published: March 11, 2013

implications of this reaction, namely those related to structural features of the conjugate bases that could be possibly formed from both isomers.

RESULTS AND DISCUSSION

Choice of the Model Chemistry. A fragment of the experimental infrared (IR) spectrum of matrix-isolated saccharin is shown in Figure 1, along with several calculated

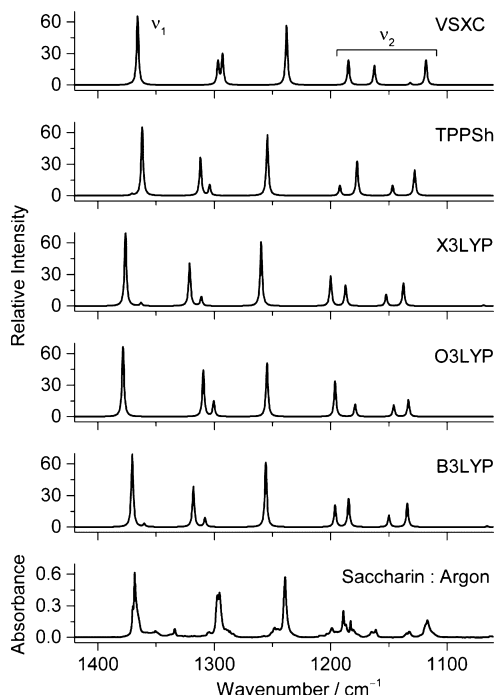


Figure 1. Fragment of the experimental infrared spectrum of saccharin isolated in an argon matrix at 15 K (bottom) compared with several simulated infrared spectra of saccharin in the region of the νSO_2 vibrations. The 6-311++G(3df,3pd) basis set was used with all the functionals. Theoretical wavenumbers are not scaled. ν_1 : νSO_2 *as*; ν_2 : mixed νSO_2 *s* + δCH modes.

spectra for this molecule. Previous combined experimental and theoretical studies on saccharin derivatives showed that, due to the SO_2 moiety, the predicted vibrational frequencies and infrared intensities are very sensitive to the theoretical approach employed. It was found that the use of cost-effective density functional theory requires basis sets including extensive polarization and diffuse functions to provide the most suitable approach in attaining reliable structural and spectroscopic predictions.^{16,17} Taking into consideration some reviews on the general performance of DFT functionals,¹⁸ we carried out optimization of the structure followed by calculations of the vibrational spectrum of saccharin using the VSXC, O3LYP, X3LYP, and TPSSH functionals together with several basis sets. The widely used B3LYP functional was also included as a reference.

The prediction of the vibrational spectrum of saccharin is especially difficult due to the presence in this molecule of both the SO_2 moiety and the aromatic ring. The antisymmetric (*as*) and symmetric (*s*) stretching (ν) vibrations of the SO_2 group in inorganic molecules and in neat SO_2 isolated in cryogenic matrices occur around 1400 and 1200 cm^{-1} , respectively.¹⁹ On the other hand, in aromatic molecules, the CH in-plane bending (δ) vibrations fall within the 1200–1100 cm^{-1} range.²⁰

In saccharin, νSO_2 *s* and four δCH vibrations occur at similar frequencies. The precise theoretical frequencies of these vibrations and their mixing pattern in the ν_2 range (see Figure 1) are very sensitive to the calculated equilibrium geometry.

Figure 2 shows the calculated values obtained at different levels of approximation in this study for selected geometrical

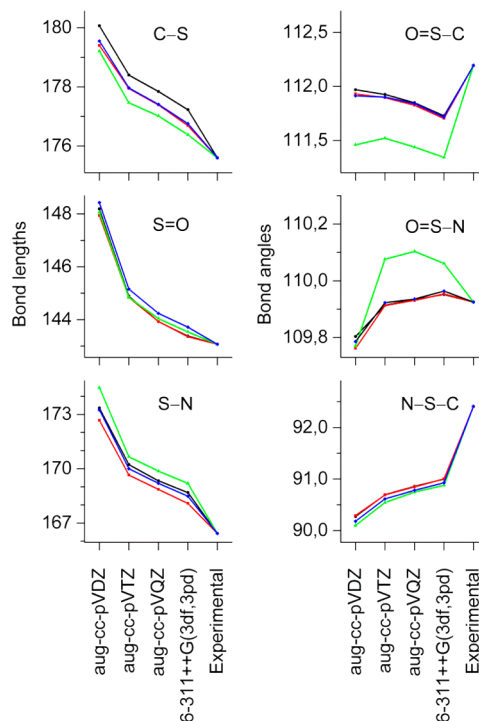


Figure 2. Selected geometrical parameters (bond lengths in pm and bond angles in degrees) calculated with the O3LYP (red), VSXC (green), TPSSH (blue), and B3LYP (black) functionals and different basis sets. Experimental data from ref 21.

parameters, compared with experimental values obtained from X-ray diffraction studies.²¹ The experimental geometries refer to the crystal structure, where saccharin forms centrosymmetric dimers stabilized by two $\text{C}=\text{O}\cdots\text{H}-\text{N}$ intermolecular hydrogen bonds. In this way, the $\text{HNC}=\text{O}$ moiety of saccharin crystal becomes more distorted comparing to a monomer in vacuum, while the geometry of the SO_2 fragment is less affected by crystal packing forces. Even though the calculations refer to isolated molecules in vacuo, the comparison with X-ray structures still appears very instructive. For example, the presence of a considerable number of polarization functions in the basis set for the accurate reproduction of bond lengths and angles where hypervalent sulfur atoms are involved is shown to be very important. It is also evident that the 6-311++G(3df,3pd) Pople-type basis set outperforms (in particular, for bond lengths) the more demanding Dunning-type aug-cc-pVTZ and aug-cc-pVQZ basis sets for this particular system, whichever functional was used (see Figure 2).

The quality of different DFT functionals combined with the 6-311++G(3df,3pd) basis set was then evaluated regarding their ability to predict vibrational data. A set of well-defined bands in the infrared spectrum of matrix-isolated saccharin (see Figure 3) was chosen, and the experimental frequencies were compared with their calculated counterparts (see Table 1). The best overall agreement was obtained for the O3LYP functional, with a mean unsigned error (MUE) of 8.55 cm^{-1} ,

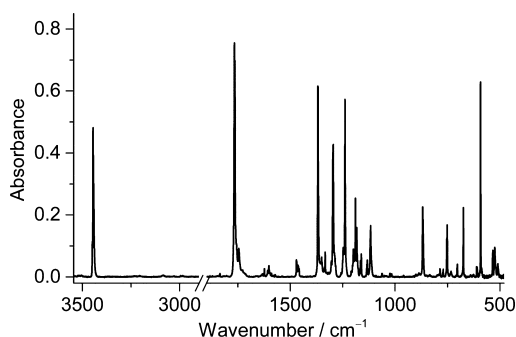


Figure 3. Experimental spectrum of monomeric saccharin isolated in argon at 15 K.

Table 1. Experimental and Theoretical Frequencies in the Infrared Spectrum of Saccharin Used in the Calculation of the Mean Unsigned Errors (MUE)

Ar (15 K) ^a	calculated/cm ⁻¹				
	VSXC	TPSSh	X3LYP	O3LYP	B3LYP
1765.8	1774.8	1784.7	1808.2	1801.7	1801.0
1471.5	1479.4	1491.2	1499.1	1483.5	1495.8
1463.3	1468.1	1482.9	1491.2	1473.1	1487.8
1368.4	1372.6	1370.8	1376.4	1378.4	1370.5
1239.1	1237.9	1254.4	1259.8	1254.7	1255.7
1132.7	1131.6	1146.9	1152.4	1145.9	1149.9
1116.7	1118.1	1127.9	1137.5	1133.2	1134.2
868.4	823.2	851.3	860.6	860.9	855.8
786.1	785.4	794.9	805.5	791.7	803.0
770.4	762.1	768.7	778.7	767.2	776.3
751.6	749.7	753.6	767.7	752.0	764.7
703.2	693.5	700.3	712.1	702.7	709.8
674.5	669.6	669.2	685.6	671.8	681.4
608.7	600.2	608.5	619.5	613.0	617.6
592.4	569.4	581.0	592.9	587.3	590.6
533.1	521.3	526.4	539.0	528.8	537.0
524.4	514.1	520.6	528.3	522.9	526.6
509.3	494.9	501.3	511.0	503.3	509.0
MUE/cm ⁻¹	9.33	9.39	14.54	8.55	12.05

^aThe experimentally observed band due to the NH stretching vibration of saccharin appears at 3445.8 cm⁻¹. This band was not used in the estimation of MUEs.

closely followed by the VSXC and TPSSh functionals, with MUEs of 9.33 and 9.39 cm⁻¹, respectively. The B3LYP functional shows a MUE of 12.05 cm⁻¹, while the largest deviation from the experiment was found for X3LYP (14.54 cm⁻¹). After consideration of all the different functionals and basis sets, the O3LYP/6-311++G(3df,3pd) level of theory arose as the best approach to be used in the vibrational characterization of new structures that might be generated from saccharin in the photochemical experiments. Also, along with the best overall agreement for the calculated frequencies, the O3LYP/6-311++G(3df,3pd) method reproduces the infrared intensities of the vibrational modes fairly well.

Narrow-Band UV-Induced Photochemistry of Matrix-Isolated Saccharin: First Observation of Iso-saccharin. In the present study, matrix-isolated saccharin was irradiated with narrow-band UV light provided by an optical parametric oscillator. Preliminary selection of the wavelength for the applied UV light was guided by the absorption spectrum of saccharin in ethanol.²² The series of UV irradiations of matrix-

isolated saccharin in the present study started at $\lambda = 300$ nm and continued at shorter wavelengths. After each irradiation, the reaction was monitored by analysis of the IR spectrum. The first phototransformations were observed for $\lambda = 295$ nm, and the effect became more pronounced when irradiation was performed at 290 nm. Upon these irradiations, the bands due to saccharin decreased in intensity, whereas a new set of bands at 1718.1, 1398.7, 1218.6, 973.4, 858.6, 800.5, 768.6, 607.2, and 553.2 cm⁻¹ emerged in the spectrum (Figure 4a). The IR spectrum of the photoproduct consists of sharp absorption bands, as narrow as the bands in the initial IR spectrum, which suggests occurrence of a photoisomerization.

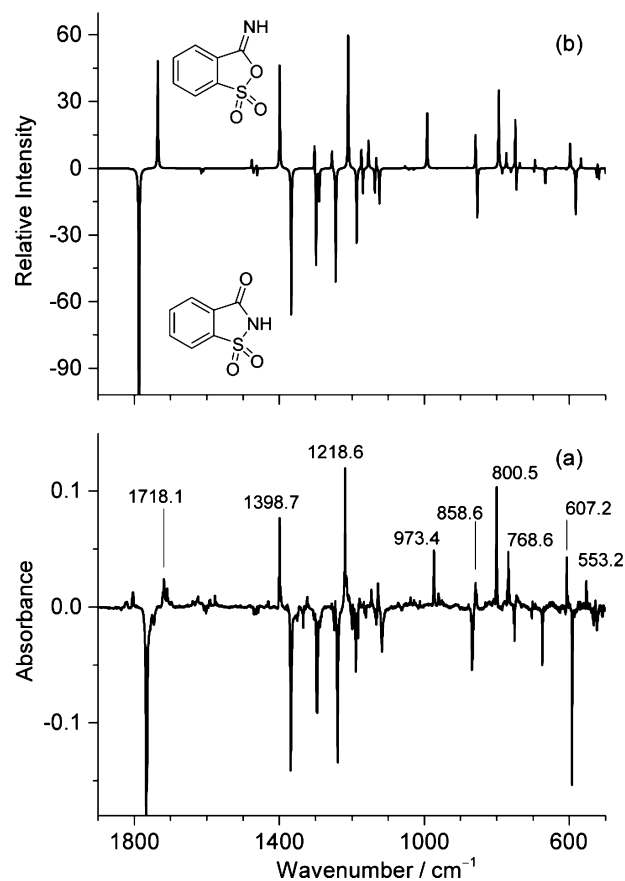


Figure 4. Difference infrared spectrum, obtained by subtraction of the spectrum recorded after the matrix deposition (negative bands) from the spectrum recorded after UV ($\lambda = 290$ nm; 78 min) irradiation (positive bands) of matrix-isolated saccharin (a), compared with the theoretical one obtained by subtraction of the simulated spectrum of saccharin from iso-saccharin (b). Theoretical wavenumbers were scaled by a factor of 0.992 obtained by least-squares linear fitting. In the simulation, the calculated intensities of iso-saccharin were scaled by 0.7.

Heterocyclic molecules bearing the HNC=O moiety, which is also present in saccharin, have been found to frequently undergo oxo-hydroxy photoisomerization.²³ On the other hand, as stated above,¹⁴ other conceptually possible isomerizations in saccharin may result from an oxygen atom shift from SO₂ to form *N*-hydroxysulfonamide or from homolysis of the S–N bond. The structures of these putative photoproducts were optimized in the present study and their vibrational spectra subsequently calculated at the O3LYP/6-311++G(3df,3pd) level of theory. These geometries and calculated spectra are

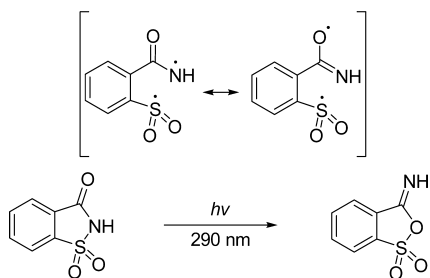
available in the Supporting Information (Scheme S1). After comparing the experimental difference IR spectrum (Figure 4a) with the simulated difference spectra built from saccharin and item-by-item examination of putative products, it could doubtlessly be concluded that the photoproduct bands indicate the formation of 3-imino-3H-2,1-benzoxathiole-1,1-dioxide (figure 4b), which we designate for brevity as “iso-saccharin”.

It can be estimated that about 70% of the consumed reactant has been converted to iso-saccharin (see Figure 4), while the remaining consumed material undergoes photofragmentation. Observation, in the spectrum of the irradiated matrix, of characteristic absorption bands due to an O=C=N moiety around 2260–2240 cm^{-1} (see Figure S2, Supporting Information) suggests isocyanic acid or its derivatives as possible fragmentation photoproducts of saccharin. It is known that the antisymmetric O=C=N stretching vibration falls in this spectral range and the corresponding infrared intensity is huge (800–1100 km mol^{-1}).^{24,25}

It is also interesting to comment on the nature of the electronic states involved in the excitation of saccharin at 290 nm. In the experimental spectrum,²² a very weak oscillator strength can be observed around 290 nm, suggesting that this low intensity absorption is associated with an $n\pi^*$ transition. Time-dependent DFT (TD-DFT) calculations performed at the O3LYP/6-311++G(3df,3pd) level show that the first (vertical) excited singlet state of saccharin has a very low oscillator strength ($f = 0.0000$; at this level it does not have any significant digits in the standard Gaussian output) and is located at 293.62 nm, in excellent agreement with the onset of the photochemistry observed in this work. Moreover, natural bond orbital (NBO) calculations show that the HOMO and the LUMO of saccharin correspond to the lone-pair n orbital and the π^* orbital of the carbonyl group, respectively (see Figure S3, Supporting Information). Thus, all the experimental and theoretical data indicate that the observed isomerization is originated by the $n\pi^*$ excitation of the carbonyl moiety.

The proposed mechanism for the observed unprecedented photoisomerization of the saccharin system involves photo-induced homolysis of the S–N bond, producing a delocalized biradicaloid in the amide moiety that, upon rotation around the exocyclic C–C bond, affords the iso-saccharin product through ring closure (Scheme 3). A similar biradicaloid rearrangement

Scheme 3. Photoisomerization Reaction Observed for Saccharin

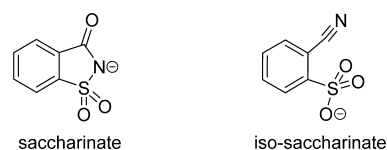


was recently proposed to take place in the photochemical conversion of diketene into cyclobutane-1,3-dione,²⁶ also occurring in argon matrices upon an $n\pi^*$ excitation of the reactant.

Structures of the Saccharinate and Iso-saccharinate Anions: Relevance to the Photochemistry of Saccharin. It is recognized that the saccharinate conjugate base, obtained

by deprotonation of the NH moiety in saccharin, is a very versatile and polyfunctional ligand in coordination chemistry.⁷ Here, we calculated the structures of the conjugate bases that result from deprotonation of both isomers, saccharin and iso-saccharin. Their optimized geometries are given in the Supporting Information. The saccharinate anion resembles very much its precursor, saccharin, and is a stable minimum in the calculations. On the contrary, deprotonation of the NH group in iso-saccharin induces barrierless cleavage of the CO bond, the resulting anion consisting of the cyano- and SO_3 groups linked to the aromatic ring at vicinal positions (formally 2-cyanobenzene sulfonate; Chart 1). To the best of our knowledge, 2-cyanobenzene sulfonate was never considered as a photoproduct of saccharin derivatives nor has it been described in the literature.

Chart 1. Structures of Saccharinate and Iso-saccharinate Anions (Conjugate Bases)



Interestingly, on moving from the neutral to anionic species, the iso-saccharinate becomes strongly stabilized compared to the saccharinate. The relative free energy of iso-saccharin (at room temperature) decreases from 50.8 (neutral) to 7.3 (anion) kJ mol^{-1} only, calculated for monomers in vacuum. Taking into account that calculated net dipole moments of saccharinate and iso-saccharinate are 8.04 and 9.35 D, respectively, one could expect that the more polar iso-saccharinate will be further stabilized in polar environments,²⁷ such as ionic liquids.^{8–11} An exhaustive search of the online molecule databases did not retrieve any record for the iso-saccharin or its conjugate base; neither could we find any reference to these structures in the literature.

CONCLUSIONS

In this study, we have shown that saccharin undergoes structural rearrangement when subjected to narrow-band ultraviolet ($\lambda = 290 \text{ nm}$) irradiation. The observed photoisomerization begins with an $n\pi^*$ excitation of the carbonyl moiety of the saccharin system and involves the homolysis of the S–N bond, generating a delocalized biradicaloid, which subsequently undergoes internal rotation and after ring closure produces the rearranged product. This photoisomerization of saccharin to iso-saccharin, never reported before, may have implications in the uses of saccharin, in particular when deprotonation is facilitated. In those cases, the present study shows that the iso-saccharinate anion (conjugate base) shall be promptly converted into 2-cyanobenzene sulfonate in a barrierless process. These changes in structure of the components shall imply important alterations in the properties of the saccharin- or saccharinate-based materials, in particular, the recently proposed saccharin-based ionic liquids.

EXPERIMENTAL AND COMPUTATIONAL METHODS

Samples were prepared by heating saccharin in a miniature glass oven placed inside the vacuum chamber of a cryostat and then depositing the saccharin vapors with a large excess of argon onto a CsI window

cooled to 15 K. Narrow-band (fwhm $\sim 0.2\text{ cm}^{-1}$) UV irradiation was provided by the frequency-doubled signal beam of a Quanta-Ray MOPO-SL optical parametric oscillator, pumped with a pulsed Nd:YAG laser (repetition rate 10 Hz, pulse energy $\sim 3\text{ mJ}$). Commercial saccharin (99%, Aldrich) and argon (N60, Air Liquide) were used.

All calculations were performed with the Gaussian 09 program package, and functionals and basis sets were applied as defined in Gaussian.²⁸ The equilibrium geometries reported here were optimized within the C_s symmetry point group, where applicable. The harmonic vibrational frequencies were then calculated at the optimized geometry. The nature of the obtained stationary points as true minima on the potential energy surface was confirmed through the analysis of the corresponding Hessian matrix.

■ ASSOCIATED CONTENT

■ Supporting Information

Figure S1, showing the 1900–600 cm^{-1} region (an extension of Figure 1 to the whole fingerprint region); Figure S2, an extended version of Figure 4 showing the complete mid-IR region; Figure S3 showing the calculated frontier natural bond orbitals of saccharin; Scheme S1, showing structures of saccharin, iso-saccharin, and other isomeric forms considered in the analysis of the vibrational spectrum of the observed photoproduct; Tables S1 and S2, showing structures of anions derived from saccharin and iso-saccharin, optimized at the O3LYP/6-311++G(3df,3pd) level of theory, with Cartesian coordinates and APT charges. This material is available free of charge via the Internet at <http://pubs.acs.org>.

■ AUTHOR INFORMATION

Corresponding Author

*E-mail: reva@qui.uc.pt

Notes

The authors declare no competing financial interest.

■ ACKNOWLEDGMENTS

This work was supported by the Portuguese “Fundação para a Ciência e a Tecnologia” (FCT) Research Projects PTDC/QUI-QUI/111879/2009 and PTDC/QUI-QUI/118078/2010, FCOMP-01-0124-FEDER-021082, cofunded by QREN-COMPETE-UE, and PEst-C/MAR/LA0015/2011. L.D. acknowledges FCT for the doctoral grant (No. SFRH/BD/62090/2009).

■ REFERENCES

- (1) George, V.; Arora, S.; Sharma, V.; Wadhwa, B. K.; Singh, A. K. *Food Bioprocess Technol.* **2010**, *5*, 323–330.
- (2) Wepplo, P. J.; Rampulla, R. A.; Heffernan, G. D.; Cossette, M. V.; Langevine, C. M.; Kameswaran, V.; Diehl, R. E.; Fiordeliso, J. J.; Haley, G. J.; Guaciaro, M. A. Herbicidal 3-heterocyclic Substituted Benzisothiazole and Benzisoxazole Compounds. US Patent US6706663 2004.
- (3) Wang, L. H.; Yang, X. Y.; Zhang, X.; Mihalic, K.; Fan, Y.-X.; Xiao, W.; Howard, O. M. Z.; Appella, E.; Maynard, A. T.; Farrar, W. L. *Nat. Med.* **2004**, *10*, 40–47.
- (4) Qiao, N.; Li, M.; Schlindwein, W.; Malek, N.; Davies, A.; Trappitt, G. *Int. J. Pharm.* **2011**, *419*, 1–11.
- (5) Ahn, K.; Baek, H.; Lee, S.; Cho, C. *J. Org. Chem.* **2000**, *65*, 7690–7696.
- (6) Baran, E. J.; Yilmaz, V. T. *Coord. Chem. Rev.* **2006**, *250*, 1980–1999.
- (7) Baran, E. J. *Quim. Nova* **2005**, *28*, 326–328.
- (8) Quentel, F.; Stankoska, K.; Grupče, O.; Jovanovski, G.; Mirčeski, V. *Electrochem. Commun.* **2011**, *13*, 1476–1478.

- (9) Zhang, Q.; Liu, S.; Li, Z.; Li, J.; Chen, Z.; Wang, R.; Lu, L.; Deng, Y. *Chem.—Eur. J.* **2009**, *15*, 765–778.
- (10) Carter, E. B.; Culver, S. L.; Fox, P. A.; Goode, R. D.; Ntai, I.; Tickell, M. D.; Traylor, R. K.; Hoffman, N. W.; Davis, J. H., Jr. *Chem. Commun.* **2004**, 630–631.
- (11) Shkrob, I. A.; Marin, T. W.; Chemerisov, S. D.; Hatcher, J.; Wishart, J. F. *J. Phys. Chem. B* **2012**, *116*, 9043–9055.
- (12) Ono, I.; Sato, S.; Fukuda, K.; Inayoshi, T. *Bull. Chem. Soc. Jpn.* **1997**, *70*, 2051–2055.
- (13) Kamigata, N.; Saegusa, T.; Fujie, S.; Kobayashi, M. *Chem. Lett.* **1979**, 9–12.
- (14) Döpp, D. *Int. J. Photoenergy* **2001**, *3*, 41–48.
- (15) Cho, D. W.; Oh, S. W.; Kim, D. U.; Park, H. J.; Xue, J. Y.; Yoon, U. C.; Mariano, P. S. *Bull. Korean Chem. Soc.* **2010**, *31*, 2453–2458.
- (16) Kaczor, A.; Almeida, R.; Gómez-Zavaglia, A.; Cristiano, M. L. S.; Fausto, R. *J. Mol. Struct.* **2008**, *876*, 77–85.
- (17) Almeida, R.; Gómez-Zavaglia, A.; Kaczor, A.; Ismael, A.; Cristiano, M. L. S.; Fausto, R. *J. Mol. Struct.* **2009**, *938*, 198–206.
- (18) Sousa, S. F.; Fernandes, P. A.; Ramos, M. J. *J. Phys. Chem. A* **2007**, *111*, 10439–10452.
- (19) Zeng, X.; Beckers, H.; Neuhaus, P.; Grote, D.; Sander, W. Z. *Anorg. Allg. Chem.* **2012**, *638*, 526–533.
- (20) Giuliano, B. M.; Reva, I.; Lapinski, L.; Fausto, R. *J. Chem. Phys.* **2012**, *136*, 024505.
- (21) Wardell, J. L.; Low, J. N.; Glidewell, C. *Acta Crystallogr., Sect. E: Struct. Rep. Online* **2005**, *61*, o1944–o1946.
- (22) Berci-Filho, P.; Quina, F. H.; Gehlen, M. H.; Politi, M. J.; Neumann, M. G.; Barros, T. C. I. *J. Photochem. Photobiol., A* **1995**, *92*, 155–161.
- (23) See, for example, Scheme 2 in: Reva, I.; Almeida, B. J. A. N.; Lapinski, L.; Fausto, R. *J. Mol. Struct.* **2012**, *1025*, 74–83.
- (24) Reva, I.; Lapinski, L.; Fausto, R. *J. Mol. Struct.* **2010**, *976*, 333–341.
- (25) Teles, J. H.; Maier, G.; Hess, B. A., Jr.; Schaad, L. J.; Winnewisser, M.; Winnewisser, B. P. *Chem. Ber.* **1989**, *122*, 753–766.
- (26) Breda, S.; Reva, I.; Fausto, R. *J. Phys. Chem. A* **2012**, *116*, 2131–2140.
- (27) Jakopin, Z.; Dolenc, M. S. *Curr. Med. Chem.* **2010**, *17*, 651–671.
- (28) Gaussian 09, Revision A.02: Frisch, M. J.; Trucks, G. W.; Schlegel, H. B.; Scuseria, G. E.; Robb, M. A.; Cheeseman, J. R.; Scalmani, G.; Barone, V.; Mennucci, B.; Petersson, G. A.; Nakatsuji, H.; Caricato, M.; Li, X.; Hratchian, H. P.; Izmaylov, A. F.; Bloino, J.; Zheng, G.; Sonnenberg, J. L.; Hada, M.; Ehara, M.; Toyota, K.; Fukuda, R.; Hasegawa, J.; Ishida, M.; Nakajima, T.; Honda, Y.; Kitao, O.; Nakai, H.; Vreven, T.; Montgomery, J. A., Jr.; Peralta, J. E.; Ogliaro, F.; Bearpark, M.; Heyd, J. J.; Brothers, E.; Kudin, K. N.; Staroverov, V. N.; Kobayashi, R.; Normand, J.; Raghavachari, K.; Rendell, A.; Burant, J. C.; Iyengar, S. S.; Tomasi, J.; Cossi, M.; Rega, N.; Millam, J. M.; Klene, M.; Knox, J. E.; Cross, J. B.; Bakken, V.; Adamo, C.; Jaramillo, J.; Gomperts, R.; Stratmann, R. E.; Yazyev, O.; Austin, A. J.; Cammi, R.; Pomelli, C.; Ochterski, J. W.; Martin, R. L.; Morokuma, K.; Zakrzewski, V. G.; Voth, G. A.; Salvador, P.; Dannenberg, J. J.; Dapprich, S.; Daniels, A. D.; Farkas, O.; Foresman, J. B.; Ortiz, J. V.; Cioslowski, J.; Fox, D. J. Gaussian, Inc., Wallingford, CT, 2009.